

Characterization of subcell open-circuit voltages in InGaP/GaAs tandem solar cells fabricated using hydride vapor phase epitaxy

Taketo Aihara, Takeshi Tayagaki, Ryuji Oshima, Yasushi Shoji, Kikuo Makita, and Takeyoshi Sugaya

National Institute of Industrial Science and Technology (AIST)
Umezono, Tukuba, Ibaraki 305-8568, Japan
E-mail: aihara-t@aist.go.jp

Abstract

We report subcell open-circuit voltages of InGaP/GaAs tandem solar cells fabricated using hydride vapor phase epitaxy. By using the spectral reciprocity relation between the electroluminescence and the quantum efficiency, the current-voltage characteristics of the individual subcells have been derived from measurements of the electroluminescence peak intensity as a function of the electroluminescence injection current. Combined with implied short-circuit current extracted from the external quantum efficiency measurements, the individual subcell open-circuit voltages are extracted.

1. Introduction

As highest efficiency photovoltaic devices, III–V solar cells have attracted much attentions. The highest conversion efficiencies have been achieved in multijunction solar cells under concentration [1,2]. In addition, InGaP/GaAs dual-junction solar cells (DJSCs) and their modules have been investigated extensively as a practical thin film photovoltaic device owing to their excellent bandgap combination in lattice-match systems, exhibiting a conversion efficiency (η) of 31.6% [3]. Even though the devices have shown excellent solar cell performances, the use of III–V devices are limited only to high-value applications, such as space and high-concentration systems, owing to their high manufacturing cost that arises from the utilization of industry standard metal–organic vapor phase epitaxy (MOVPE). To extend the use of III–V solar cells, manufacturing cost reductions is a crucial issue.

Recently, hydride vapor phase epitaxy (HVPE) has gained much attentions as a low-cost alternative for the fabrication of III–V solar cells. HVPE utilizes cost-effective group-III metals and provides a higher growth rate of several hundred $\mu\text{m}/\text{h}$, hence decreasing the manufacturing cost. In the previous works, we have fabricated InGaP / GaAs DJSCs using the HVPE method [4]. To boost the performance, further insight of the obtained solar cell properties such as open-circuit voltage (V_{oc}) are required. Electroluminescence (EL) measurements have been used to obtain the subcell V_{oc} with external quantum efficiency (EQE) based on Rau's reciprocity relation [5–7].

In this study, we investigate the subcell V_{oc} of the InGaP/GaAs DJSCs. The current-voltage (I-V) characteristics of each subcell are investigated in detail. Combined with im-

plied short-circuit current extracted from the external quantum efficiency measurements, the individual subcell V_{oc} are extracted.

2. Experimental procedure

InGaP/GaAs DJSCs were grown on 2-inch diameter GaAs (001) substrates miscut 4° toward the (111)B direction in a custom-built hot-wall reactor (Taiyo Nippon Sanso, H260) at atmospheric pressure [8,9]. The source and substrate regions were heated to 850°C and 660°C , respectively. Gaseous hydrogen chloride (HCl), gallium (Ga) and indium (In) metals, arsine (AsH_3), and phosphine (PH_3) were utilized to grow III–V layers. Dimethylzinc (DMZn) and hydrogen sulfide (H_2S) were utilized as the p- and n-type dopants, respectively. The growth rates of GaAs and InGaP were 8 and $30^\circ\text{m}/\text{h}$, respectively, and the total flow rate of the H_2 -carrier gas was 6 SLM. The InGaP/GaAs DJSC structure is shown in Fig. 1. After the HVPE growth of the device structures, AuGeNi/Au and Ti/Au electrodes were formed as n- and p-type ohmic contacts using electron-beam evaporation. Mesa isolation was performed using a standard photolithography system. SiO_2 (110 nm)/ TiO_2 (50 nm) antireflection coating (ARC) was deposited onto the cell via radio-frequency magnetron sputtering. The cell size was 0.1024 cm^2 .

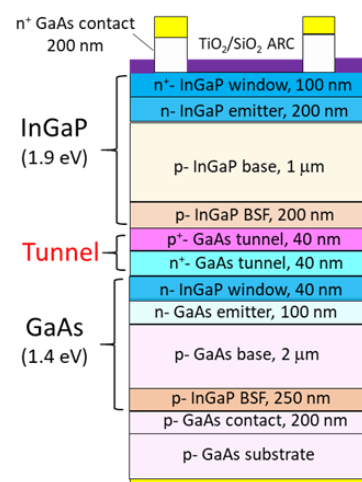


Fig. 1 Schematic of the InGaP/ GaAs dual-junction solar cell.

The EQE was measured with a chopped, monochromatic light with a constant photon flux of $1 \times 10^{14} \text{ cm}^{-2}$. The current–voltage characteristics were measured under an air mass of 1.5 global (AM1.5G) with illumination of 1 -Sun. For the EL intensity measurements, the current is injected by tuning applied voltage to devices using the source meter (Keithley 2604B). Luminescence signals are detected by a charge-coupled device.

3. Results and discussion

Figure 2 (a) shows I-V curves under an AM1.5G at 1 Sun and dark conditions. The DJSC yielded an η value of 14.0% at 1 sun with short-circuit current (J_{sc}): 6.88 mA/cm^2 , V_{oc} : 2.36 V, and fill factor: 0.86. The V_{oc} has a sufficient large value that is expected from the bandgap energies of InGaP and GaAs subcells. On the other hand, the J_{sc} tends to be lower than expected value [4].

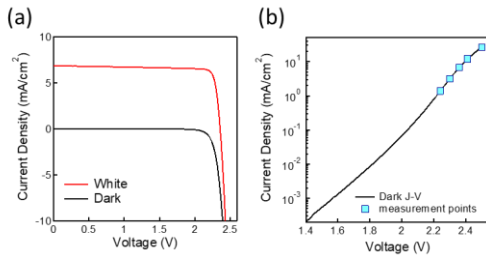


Fig. 2(a) Light (red) and Dark (black) current-voltage curves of the InGaP/GaAs dual-junction solar cell. (b) Dark current-voltage curve on log scale for the InGaP/GaAs dual-junction solar cell. The square markers indicate the points of the injection-current in the EL measurement.

Figure 2 (b) shows I-V curve under dark condition in a log-linear scale. The markers indicate the applied voltage for EL measurements. We used the voltages, in which the current density is comparable to the J_{sc} obtained in current-voltage measurements under 1Sun illuminated condition.

Figure 3 (a) shows EL spectra measured at different injection current conditions. The luminescence signals at 1.4 and 1.9 eV correspond to the GaAs and InGaP, respectively. The luminescence intensity increases with injection current both for InGaP and GaAs subcells. Figure 3(b) shows EQE spectra for InGaP and GaAs subcells. Figure 3(c) shows EL peak intensities as a function of the injection current for InGaP and GaAs subcells. Figure 3(d) shows extracted current-voltage characteristics of the InGaP (blue) and GaAs (green) subcells and summation (red). The current-voltage characteristics of each subcell are derived following the procedure reported in previous papers [5,6]. Combined with implied short-circuit currents extracted from EQE measurements, the individual subcell V_{oc} are extracted as 1412 and 948 meV for the InGaP and GaAs subcells, respectively. The obtained V_{oc} for the InGaP subcell is a little larger than that of InGaP single-junction devices of 1350 meV reported in the previous paper [10]. This implies that the radiative recombination efficiencies are reduced in the GaAs subcells compared to the InGaP subcells. In fact, when we assume the smaller radiative recombination

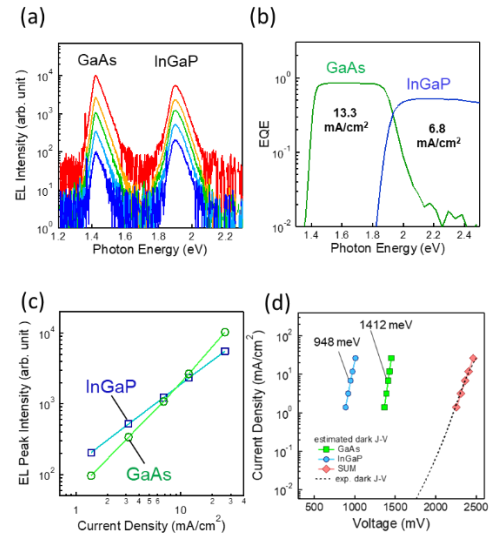


Fig. 3(a) EL spectra measured at different injection current conditions. (b) EQE spectra for the InGaP (blue) and GaAs (green) sub-cells. (c) EL peak intensity as a function of the injection current for InGaP and GaAs subcells. (d) Estimated current-voltage characteristics of the InGaP (blue) and GaAs (green) sub-cells and summation (red). The dash line indicates the current-voltage curve under dark condition.

of GaAs subcells of 1 % of that in InGaP subcell, the V_{oc} of InGaP and GaAs subcells are estimated as 1352 and 1008 meV, respectively, which is consistent with the previous paper. Further studies are required to determine the precise V_{oc} values in InGaP/GaAs dual-junction devices.

4. Conclusions

We extracted the subcell V_{oc} of InGaP/GaAs DJSC fabricated using hydride vapor phase epitaxy from measurements of the EL peak intensity as a function of the EL injection current. Combined with implied short-circuit current extracted from the EQE measurements, the individual subcell V_{oc} were extracted.

Acknowledgements

This work was supported by the New Energy and Industrial Technology Development Organization (NEDO) under the Ministry of Economy, Trade and Industry (METI).

References

- [1] F. Dimroth, *et al.*, IEEE Journal of Photovoltaics, **6**, 343 (2016).
- [2] R. M. France, *et al.*, IEEE Journal of Photovoltaics, **4**, 190, (2014).
- [3] B. M. Kayes, *et al.*, IEEE Journal of Photovoltaics, **4**, 729, (2014).
- [4] R. Oshima, *et al.*, abstract PVCS IEEE.
- [5] T. Kirchartz, *et al.*, Appl. Phys. Lett. **92**, 123502 (2008).
- [6] S. Roensch, *et al.*, Appl. Phys. Lett. **98**, 251113 (2011).
- [7] C. Karcher, *et al.*, Prog. Photovoltaics **22**, 757 (2014).
- [8] R. Oshima, *et al.*, Jpn. J. Appl. Phys., **57**, 08RD06 (2018).
- [9] R. Oshima, *et al.*, IEEE Journal of Photovoltaics, **9**, 154, (2019).
- [10] Y. Shoji, *et al.*, Appl. Phys. Express **12**, 052004 (2019)